Journal of Neurotrauma
39:1495-1506 (November 2022)

DOI: 10.1089/neu.2021.0239

Journal of Neurotrauma

ORIGINAL ARTICLE IMAGING

Effects of White-Matter Tract Length in Sport-Related Concussion: A Tractography Study from the NCAA-DoD CARE Consortium

Sourajit M. Mustafi,[1,2] Ho-Ching Yang,[2] Jaroslaw Harezlak,[3] Timothy B. Meier,[4] Benjamin L. Brett,[4] Christopher C. Giza,[5,6] Joshua Goldman,[7] Kevin M. Guskiewicz,[8] Jason P. Mihalik,[8] Stephen M. LaConte,[9,10] Stefan M. Duma,[9] Steven P. Broglio,[11] Michael A. McCrea,[4] Thomas W. McAllister,[12] and Yu-Chien Wu[2,*]

Abstract

Sport-related concussion (SRC) is an important public health issue. White-matter alterations after SRC are widely studied by neuroimaging approaches, such as diffusion magnetic resonance imaging (MRI). Although the exact anatomical location of the alterations may differ, significant white-matter alterations are commonly observed in long fiber tracts, but are never proven. In the present study, we performed streamline tractography to characterize the association between tract length and white-matter microstructural alterations after SRC. Sixty-eight collegiate athletes diagnosed with acute concussion (24–48 h post-injury) and 64 matched contact-sport controls were included in this study. The athletes underwent diffusion tensor imaging (DTI) in 3.0 T MRI scanners across three study sites. DTI metrics were used for tract-based spatial statistics to map white-matter regions-of-interest (ROIs) with significant group differences. Whole-brain white-mater streamline tractography was performed to extract "affected" white-matter streamlines (i.e., streamlines passing through the identified ROIs). In the concussed athletes, streamline counts and DTI metrics of the affected white-matter fiber tracts were summarized and compared with unaffected white-matter tracts across tract length in the same participant. The affected white-matter tracts had a high streamline count at length of 80–100 mm and high length-adjusted affected ratio for streamline length longer than 80 mm. DTI mean diffusivity was higher in the affected streamlines longer than 100 mm with significant associations with the Brief

[1]Institute of Genetics, San Diego, California, USA.
[2]Department of Radiology and Imaging Sciences, [12]Department of Psychiatry, Indiana University School of Medicine, Indianapolis, Indiana, USA.
[3]Department of Epidemiology and Biostatistics, School of Public Health, Indiana University, Bloomington, Indiana, USA.
[4]Department of Neurosurgery, Medical College of Wisconsin, Milwaukee, Wisconsin, USA.
[5]Department of Neurosurgery, David Geffen School of Medicine at University of California, Los Angeles, Los Angeles, California, USA.
[6]Division of Pediatric Neurology, Mattel Children's Hospital, University of California, Los Angeles, Los Angeles, California, USA.
[7]Family Medicine, Ronald Reagan UCLA Medical Center, UCLA Health - Santa Monica Medical Center, Los Angeles, California, USA.
[8]Matthew Gfeller Sport-Related Traumatic Brain Injury Research Center, Department of Exercise and Sport Science, University of North Carolina, at Chapel Hill, Chapel Hill, North Carolina, USA.
[9]School of Biomedical Engineering and Sciences, Wake-Forest and Virginia Tech University, Blacksburg, Virginia, USA.
[10]Virginia Tech Carilion Research Institute, Roanoke, Virginia, USA.
[11]Michigan Concussion Center, School of Kinesiology, University of Michigan, Ann Arbor, Michigan, USA.

*Address correspondence to: *Yu-Chien Wu, MD, PhD, DABMP, Department of Radiology and Imaging Sciences, Indiana University School of Medicine, 355 West 16th Street, Suite 4100, Indianapolis, IN 46202, USA E-mail:* yucwu@iu.edu

Symptom Inventory score. Our findings suggest that long fibers in the brains of collegiate athletes are more vulnerable to acute SRC with higher mean diffusivity and a higher affected ratio compared with the whole distribution.

Keywords: CARE Consortium; sport-related concussion; diffusion tensor imaging; tract length; tractography; white matter

Introduction

Sport-related concussion (SRC) is the mildest form of traumatic brain injury (TBI) with approximately 1.6 to 3.8 million annual incidents occurring annually.[1,2] Despite the misleading term ''mild,'' athletes sustaining SRC may develop long-term sequalae with post-traumatic headache, psychological distress, cognitive impairment, and learning deficits.[3,4] These long-term sequalae often severely impact the quality of life and sabotage rehabilitative efforts. Further, concussed athletes may also be at increased risk for future concussion,[5] neurodegenerative disorders,[6] and chronic traumatic encephalopathy.[7,8]

Brain injury involves multiple tiers of mechanical forces causing immediate local damage and diffuse axonal injury.[9,10] Diffuse axonal injury, believed to be the primary neuropathology associated with mild TBI, is characterized as widespread microscopic injuries involving physical disruption of axons/cytoskeletons and metabolic alterations in cellular/subcellular biochemistry reactions.[11–14] Following a direct head impact with a linear and rotational acceleration, the inertia force propagates through the complexly structured soft tissues of the brain with shear stress. The shear wave induces physical strain and stretch on the brain tissues.[15,16] It is plausible that the level of tissue vulnerability to the effects of mechanical impacts depends on tissue's micro-and macrostructural composition. In the case of white matter, myelination may increase the dynamic modulus of axons, providing some pliability in a slow shear wave.[17,18] Nevertheless, under high, rapidly propagating shear stress, axons became stiffer and brittle as demonstrated in previous *in vitro*[18] and *in silico* studies.[17,19]

The human brain has been shown to have a varying degree of axonal myelination and micro-/macrostructure with respect to fiber length.[20] Thus, we hypothesized that the level of vulnerability of white-matter fibers will differ according to their lengths. Indeed, in previous white-matter studies of mild TBI using diffusion tensor imaging (DTI), despite variations in anatomical location, the reported significant white-matter alterations usually occurred in long fiber tracts. White-matter abnormalities are most commonly noted in the internal capsule (anterior and posterior limbs) and corona radiata (anterior, superior, and posterior).[21–29] Abnormalities are also commonly reported in the corpus callosum[21,23,27–31] and the longitudinal fasciculus.[22,24,26,27,29,32] The collective findings are intriguing regarding the less-studied hypothesis of varying vulnerability of white-matter fibers with respect to their lengths.

DTI, a magnetic resonance imaging (MRI) technique, is widely used in studies of mild TBI to detect white matter-related microstructural damage.[33–39] DTI provides scalar measures that infer microstructural organization of the tissue and exhibit adequate diagnostic sensitivity to SRC.[35] The scalar metrics include fractional anisotropy (FA) describing the coherence of microstructural organization, mean diffusivity (MD) describing the averaged water diffusion freedom regardless of directionality, axial diffusivity (AD) describing the longitudinal diffusivity along the primary orientation of white-matter fibers, and radial diffusivity (RD) describing the perpendicular diffusivity of white-matter fibers. Most appealingly, DTI also provides directional information for assessing white-matter fiber connectivity via tractography.

To characterize the susceptibility of fiber tracts to brain injury with respect to tract length, this study by the Concussion Assessment, Research and Education (CARE) Consortium performed streamline tractography and extracted tract-specific features, including the DTI metrics along the fiber streamlines, streamline counts, and streamline length. We investigated how these physical features of white-matter tracts affect their susceptibility to SRC, and how these physical features modulate the associations with clinical outcomes.

Methods

Participants

The participants were recruited from a multi-site study of the natural history of concussion conducted through the National Collegiate Athletic Association-Department of Defense (NCAA-DoD) CARE Consortium Advanced Research Core (ARC). All participants received baseline clinical assessments when recruited into the CARE-ARC study. Number of previous (self-report) concussions were recorded, and participants were excluded if they had previous concussions within 6 months of the baseline assessments. Concussion events were identified and diagnosed by the research and medical staff at each site based on an evidence-based guideline,[40] which decided concussion as ''a change in brain function following a force to the head, which may be accompanied by temporary loss of consciousness, but is identified in awake individuals with

measures of neurologic and cognitive dysfunction.'' Throughout the post-injury process, concussed athletes also received clinical care by a site's medical team. All participants (including concussed and contact-control athletes) received the same clinical assessments, blood sample collection, and multi-modal MRI scans. The clinical and imaging assessments of the contact controls were yoked to the schedule of demographically matched injured athletes. More detailed study design and the power calculation of the CARE study can be found in the method article.[41]

The study sites included in this analysis are the University of North Carolina (UNC), the University of California Los Angeles (UCLA), and Virginia Tech (VT). At the time (January 2019) when the data was frozen, there were 68 collegiate athletes diagnosed with acute concussion (24–48 h post-injury) and 64 matched contact-sport controls available for analysis. All were included in the present study (Table 1). The two groups were matched with respect to age, sex, race/ethnicity, education, estimated pre-morbid level of verbal intellectual functioning (i.e., Wechsler Test of Adult Reading [WTAR[42]], number of prior concussions, years of participation, sport type, and position played. The sports included football, soccer, and lacrosse. Severity of previous concussions are listed in Supplementary Table 1 showing no significant group difference.

All participants provided informed consent approved by the Medical College of Wisconsin Institutional Review Board (IRB; protocol #PRO23196) and the Human Research Protection Office (HRPO).

Clinical assessments

Clinical assessments followed the CARE Consortium study protocol and were collected by the on-site research and medical staff.[41] The comprehensive battery of

Table 1. Participant Demographics and Clinical Assessments

	Concussed, n = 68	*Contact control, n = 64*	
Demographics	*Mean (SD) or count*	*Mean (SD) or count*	p *value*
Age (years)	19.31 (0.92)	19.36 (1.26)	0.81
Education (years)	13.63 (0.97)	13.55 (0.77)	0.64
WTAR standard score	104.61 (14.30)	106.62 (14.28)	0.43
Sex (M:F)	58:10	52:12	0.70[a]
Body mass index	27.66 (5.94)	26.18 (4.24)	0.10
Site (UCLA:UNC:VT)	27:32:9	30:28:6	0.64[a]
Sport type (Football:Soccer:Lacrosse)	44:19:5	38:20:6	0.80[a]
Years of participation in primary sports (years)	9.90 (3.60)	10.76 (3.77)	0.18
Time from injury to MRI (h)	50.45 (35.18)	na	na
Previous concussions			
No. of participants with previous concussion (0:1:2:3)	32:27:6:3	42:16:5:1	0.16[a]
No. of football players with previous concussion (0:1:2:3)	23:16:3:2	26:8:4:0	0.21[a]
No. of soccer players with previous concussion (0:1:2:3)	7:9:2:1	13:5:1:1	0.35[a]
No. of lacrosse players with previous concussion (0:1:2:3)	2:2:1:0	3:3:0:0	0.52[a]
Position			
Football (QB:C:CB:DL:WR:LB:LS:Off:RB:S:ST)	(0:1:3:9:4:10:0:6:3:7:1)	(0:0:4:9:6:10:1:4:3:0:1)	0.32[a]
Soccer (DB:FA:G:MF)	(3:6:5:5)	(5:9:0:6)	0.10[a]
Lacrosse (DB:FA:G:MF)	(2:2:0:1)	(3:2:0:1)	0.95[a]
Clinical assessments[b]			
Brief Symptom Inventory (BSI)	6.45 (7.30)	1.15 (2.28)	$\mathbf{<10^{-4}}$
Standardized Assessment of Concussion (SAC)	26.09 (2.64)	27.68 (2.05)	$\mathbf{<10^{-3}}$
Sport Concussion Assessment Tool (SCAT)			
Symptom Score	11.32 (6.38)	2.34 (3.79)	$\mathbf{<10^{-4}}$
Symptom Severity Score	27.83 (21.92)	3.43 (5.56)	$\mathbf{<10^{-4}}$
Balance Error Scoring System (BESS)	16.51 (10.49)	10.42 (5.37)	$\mathbf{<10^{-4}}$

Bold fonts indicate p value less than 0.05.

[a]Pearson's chi-square tests were used for sex, sport types, previous concussion count, and position.

[b]Assessment scores were logarithmically transformed to adjust skewness.

Two tailed t-test was used unless noted otherwise.

(M:F) = (male:female).

(0:1:2:3) = number of previous concussions.

Site abbreviations: VT, Virginia Tech; UNC, University of North Carolina; UCLA, the University of California, Los Angeles.

Position abbreviations: QB, quarterback; C, center; CB, cornerback; DL, defensive line; WR, wide receiver; LB, linebacker; LS, long snapper; Off, tight end + off guard + off tackle; RB, running back; S, safety; ST, special team (FG offense + punt return); DB, defensive back; FA, forward attack; G, goalkeeper; MF, midfielder.

MRI, magnetic resonance imaging; SD, standard deviation; WTAR, Wechsler Test of Adult Reading.

clinical outcome measures included the Standardized Assessment of Concussion (SAC)[43] to assess cognition, the Sports Concussion Assessment Tool 3 (SCAT3)[4] to assess symptoms and their severity, the Balance Error Scoring System (BESS)[44] to assess postural stability, and the Brief Symptom Inventory (BSI)[45] to assess psychological health. The BSI score was a composite score of three subcategories: BSI-soma for somatic symptoms, and BSI-anxiety and BSI-depression for evaluating affective symptoms. Thus, a total of five clinical measures were studied for associations with white-matter abnormalities along the tracts. Both the concussed and control athletes underwent the same clinical assessments on the day the MRI scans were performed.

MRI protocol

Participants underwent MRI on Siemens MAGNETOM 3.0 T Tim Trio (VT, UNC, and UCLA) or 3.0 T Prisma (UNC and UCLA) scanners across three ARC sites with a 12-channel (VT) or 32-channel (UNC and UCLA) receiver-only head coil. For anatomical imaging, high-resolution T1-weighted images ($1\,mm \times 1\,mm \times 1\,mm$) were acquired on 3.0 T MRI scanners at each site. A three-dimensional (3D) magnetization-prepared rapid gradient-echo (MPRAGE) sequence was used with repetition time (TR)/echo time (TE)/inversion time (TI) = 2300/2.98/900 msec, flip angle = 9 degrees, field of view (FOV) = 256 mm, matrix = 256×256, 176 slices, slice thickness = 1 mm. For diffusion imaging, a single-shot spin-echo echo planar imaging (SS-SE-EPI) sequence with a twice-refocused spin echo was used. The diffusion-encoding scheme comprised 30 directions at a b-value of 2000 sec/mm^2, 30 directions at a b-value of 1000 sec/mm^2, and 4 b_0 volumes (b-value = 0 sec/mm^2). One of the b_0 volumes was acquired with a reversed phase-encoding direction. Other parameters included TE/TR = 98/7900 msec, FOV = 243 mm, matrix size = 90×90, whole-brain coverage of 60 slices with a slice thickness of 2.7 mm, and an isotropic voxel size of 2.7 mm.

Care was taken to ensure the quality and stability of the diffusion MRI signal across sites. Briefly, prior to the present study, three quality assurance and control (QA/QC) related studies were performed to ensure the MRI image quality and to evaluate cross-site diffusion signal stability. These studies included physical phantom scans, traveling human phantom scans, and analyses of non-contact-sport controls across sites as described previously.[29,31,46,47]

Image processing

The diffusion image pre-processing pipelines used were the same as those employed in a previous study.[29,31] Briefly, all the raw and motion-corrected diffusion-weighted images (DWIs) were inspected by a single trained researcher (SMM). Two data sets with severe motion artifacts beyond correction were excluded and not counted toward the total sample size described above. Diffusion image processing included pre-processing followed by computation of DTI metrics and streamline tractography. The DWIs were first de-noised using the local principal component analysis approach.[48] Unlike the conventional method of de-noising by smoothing the image, the local principal component analysis de-noising approach does not sacrifice spatial resolution. With a pair of reverse-phase encoded b_0 images as reference, the DWIs were then corrected for motion, eddy current artifacts, and static-field geometric distortion using the *eddy_openmp* command provided in the FMRIB Software Library (FSL).[49] After image pre-processing, DTI metrics were computed from the first shell with a b-value of 1000 sec/mm^2 and a linear fitting algorithm using the FSL *dtifit* command. Four classic DTI metrics were computed, including FA, MD, AD, and RD.[50] To prepare for statistical analyses of group differences, maps of the DTI metrics were transformed to the standard Montreal Neurological Institute (MNI) space using Advanced Neuroimaging Tools (ANTs) non-linear registration.[51]

Whole-brain white-matter streamline tractography was performed on all shells (b-value of 1000 s/mm^2 and b-value of 2000 s/mm^2; see Supplementary Figure S1). Because only cortical-to-cortical connections were considered in this study, the white and gray matter interface was segmented to serve as starting and destination points for tractography. For each participant, the interface was derived from their T1-weighted images (see Supplementary Figure S2). Briefly, the T1-weighted images underwent brain extraction using FSL *bet*; gray matter and white matter were segmented using FSL *FAST*; the gray-matter and white-matter masks were dilated via a Gaussian kernel with a width of 1 voxel (*fslmaths*) prior to intersection (*fslmaths*) for rendering the interface; and subcortical structures were identified and removed by *fsl_anat*. In the native subject diffusion space, streamline tractography was performed using the *track* command in CAMINO software with a q-ball and spherical harmonic reconstruction for fiber orientation distribution functions.[52] Other tractography parameters were: maximum allowable fiber number per voxel = 3, anisotropy threshold = 0.5, curvature threshold = 60 degrees, step size = 0.5 mm Euler distance, and iteration = 25 to reach a total whole-brain streamline count of 10^5 per participant.

Statistical analyses

Two-tailed *t*-tests for continuous variables and Pearson's chi-square tests for categorical variables were performed to detect group differences in participants' demographics measures, previous concussion history, sport types,

positions, and clinical assessments (Table 1). Affected white-matter areas were identified via tract-based spatial statistical (TBSS) analyses. These areas were defined to have significant differences in DTI microstructural metrics in the concussed athletes compared with the contact-sport controls. Briefly, in the standard MNI space, a common whole-brain white-matter skeleton was extracted using the FSL toolbox.[53] Within the white-matter skeleton (Fig. 1, green voxels), the non-parametric permutation-based statistics employed in TBSS (i.e., the *randomise* command) were used for voxelwise statistical analysis to test for significant group differences. A threshold-free cluster enhancement[54] and 5000 permutations[55] were used in the study. White-matter voxels were deemed significant if $p < 0.05$ after adjusting for multiple comparisons by controlling family-wise error rate (FWER). General regression models were used in TBSS with diffusion metrics as the dependent variable and the group membership as the independent variable. Covariates of age, sex, site, and scanner were included to adjust these differences in means.

Significant white-matter voxels in the standard space were collected as regions-of-interest (ROIs) and reverse-transformed back to native subject diffusion space. These ROIs then served as a filter to identify those streamlines passing through the affected white-matter areas for each participant in the concussed group and the contact-sport controls. These filtered streamlines in the concussed athletes were referred to as ''affected'' white-matter tracts (Fig. 2). Streamlines passing through the whole-brain TBSS white-matter skeleton, except the significant voxels (only the green voxels in Fig. 1), were referred to as ''unaffected'' white-matter tracts. The number and length of the streamlines were summarized for affected and unaffected white-matter tracts in the concussed athletes. The DTI microstructural metrics were converted to the intrinsic coordinates of each streamline in the CAMINO software, and the diffusion metrics along streamlines were averaged.

With respect to streamline lengths, the following comparisons were assessed: (1) the affected ratio (i.e., the ratio of affected white-matter streamlines relative to the whole distribution); (2) DTI microstructural measurements along the streamlines between affected and unaffected white-matter tracts; and (3) correlations of the DTI microstructural measurements along affected white-matter tracts with the clinical assessments. Paired *t*-tests were used for comparisons between affected and unaffected white-matter tracts within a participant, and partial correlation analyses were used to evaluate the correlation of the DTI metrics with the clinical assessment scores adjusted for sites and MRI scanners. Matlab

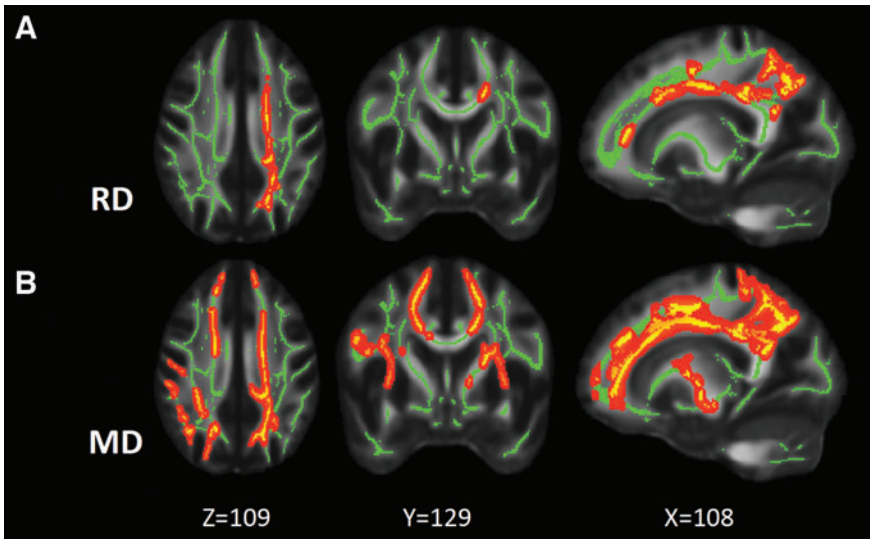

FIG. 1. Maps of white-matter voxels with significant group differences. **(A)** Maps of white-matter voxels (yellow) where the concussed athletes had significantly elevated RD compared with the contact-sport controls. **(B)** Maps of white-matter voxels where the concussed athletes had significantly elevated MD compared with the contact-sport controls. TBSS were used with a general linear model; $p < 0.05$ adjusted for multiple comparisons with the FWER was deemed significant. The green voxels denote the white-matter skeleton where the statistical test was performed. The dark red is background enhancement for illustration purposes. FWER, family-wise error rate; MD, mean diffusivity; RD, radial diffusivity; TBSS; tract-based spatial statistics.

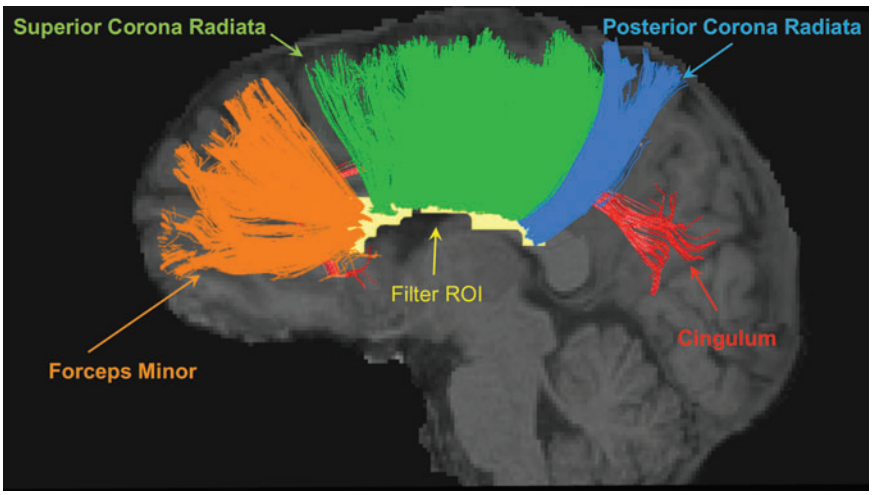

FIG. 2. Affected white-matter fiber tracts in one concussed athlete. The white-matter voxels with significant group differences in MD (i.e., yellow voxels in Fig. 1B) were collected to form an ROI in the MNI standard space. For each concussed participant, the ROI was transformed from the standard space back to the subject diffusion space, where streamline tractography was performed. Tractography streamlines passing through the filter ROI (yellow) are shown in the figure for one concussed athlete. Their corresponding white-matter tracts are the forceps minor, superior corona radiata, posterior corona radiata, and cingulum. MD, mean diffusivity; MNI, Montreal Neurological Institute; ROI, region of interest.

(The MathWorks Inc., Natick, MA, USA) and the Statistical Package for the Social Sciences (SPSS) version 24 (IBM Corp., Armonk, NY, USA) were used for plotting and statistical analyses.

Results

The characteristics of the concussed and control groups are listed in Table 1. There were no significant differences between the groups in age, education, or WTAR score ($ps > 0.43$). The sex and sport-type ratios were also not significantly different between the two groups ($ps > 0.70$, chi-square tests). At the acute concussion phase (24–48 h), the concussed group performed more poorly than the control group on all of the clinical outcome measures ($ps < 0.01$).

The TBSS analyses demonstrated significantly increased RD and MD in the concussed athletes compared with the contact-sport controls ($p < 0.05$ after controlling for FWER). White-matter voxels with significant RD and MD findings are shown in Figure 1A and 1B, respectively. The extent of the significant white-matter changes was 1936 mm^3 (i.e., 1936 1-mm^3 voxels in the MNI standard space) for RD and 4834 for MD. The extent of the white matter with MD changes encompassed the extent of the RD changes. FA and AD did not differ significantly between the groups.

The significant white-matter voxels in MD were collected to form a filter ROI (i.e., all the yellow voxels in Fig. 1B). Tractography streamlines passing through the filter ROI were clustered and their corresponding white-matter anatomies were identified as the forceps minor, superior corona radiata, posterior corona radiata, and cingulum (Fig. 2). In the concussed athletes, the mean streamline counts for the affected white matter ranged between 200 and 700 across different lengths (Fig. 3A). Whereas the 80- to 100-mm streamlines had the highest count, streamlines longer than 120 mm had the lowest count. The histogram of the affected white-matter tracts differed from that of the whole-brain white-matter-skeleton filtered streamlines, where the shortest streamlines (i.e., 20–40 mm) had the highest count (Fig. 3B). Note that the whole-brain streamline histogram included both affected and unaffected streamlines.

The next step was to assess the affected ratio (i.e., the ratio of the affected streamlines to the whole brain streamlines) with respect to streamline length. For each length category in each concussed athlete, the number of streamlines in Figure 3A was divided by the number of streamlines in Figure 3B. To correct for the inherent bias from the tract length itself, the original percentage was divided by the streamline length resulting in a length-adjusted percentage, $\%\cdot mm^{-1}$. The length-adjusted affected ratio was higher in the long fiber tracts than in the short fiber tracts (Fig. 4). For tract lengths longer than 80 mm, the affected ratio was from 0.55 to $0.65\%\cdot mm^{-1}$, compared with 0.3 to $0.4\%\cdot mm^{-1}$ in tracts shorter than 80 mm.

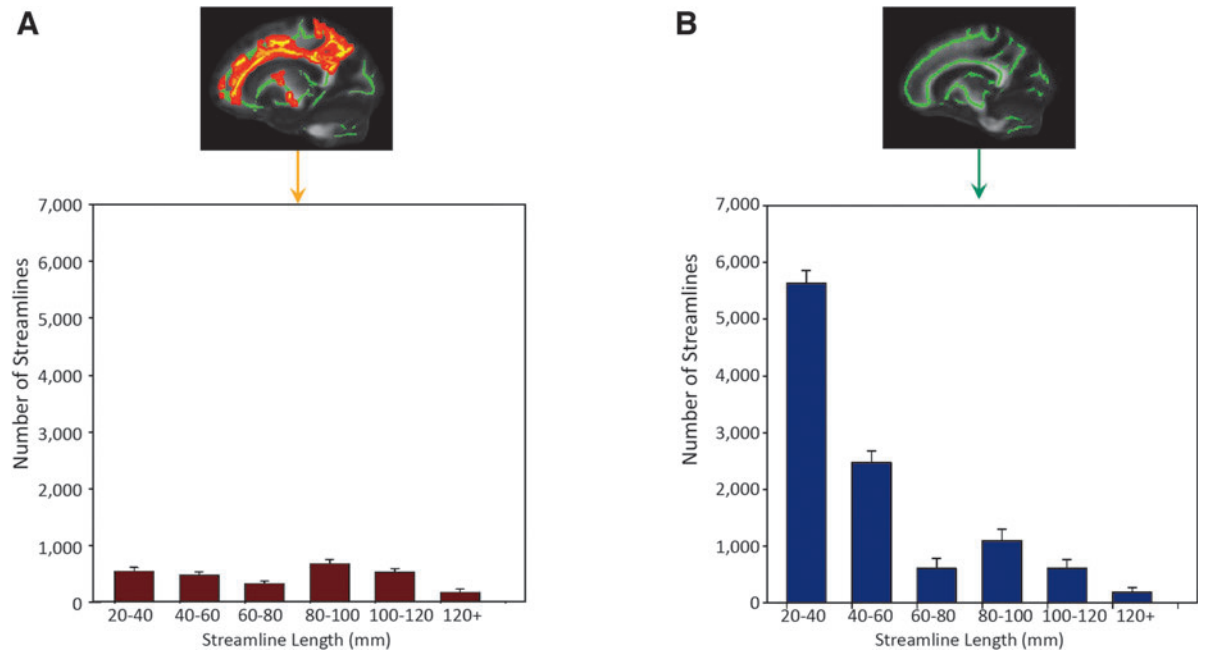

FIG. 3. Histograms of streamline counts across streamline length. **(A)** Streamline-count distribution for the affected white-matter tracts whose streamlines passed through the affected white-matter voxels (yellow voxels in the top figure). **(B)** Streamline-count distribution for whole-brain white-matter tracts whose streamlines passed through the whole-brain TBSS skeleton (green voxels in the top figure). The streamline counts in B include those streamlines in A. The bar and error bar denote the mean and standard deviation across the concussed athletes, respectively. TBSS; tract-based spatial statistics.

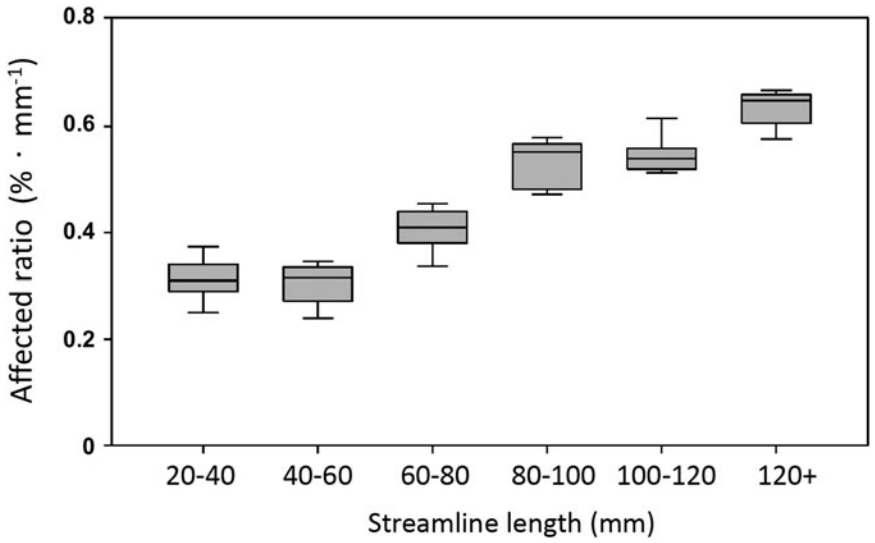

FIG. 4. Affected ratio by streamline length. The affected ratios were computed by dividing the streamline counts of affected fiber tracts in Figure 3A by the streamline counts of whole-brain skeleton-filtered fiber tracts in Figure 3B for each concussed athlete for each length category. The affected ratios were further divided by the streamline length to adjust the intrinsic bias of tract length. The box represents the 75th percentile, median, and 25th percentile of the adjusted affected ratio. The whiskers represent upper and lower extremes. No outliers were observed.

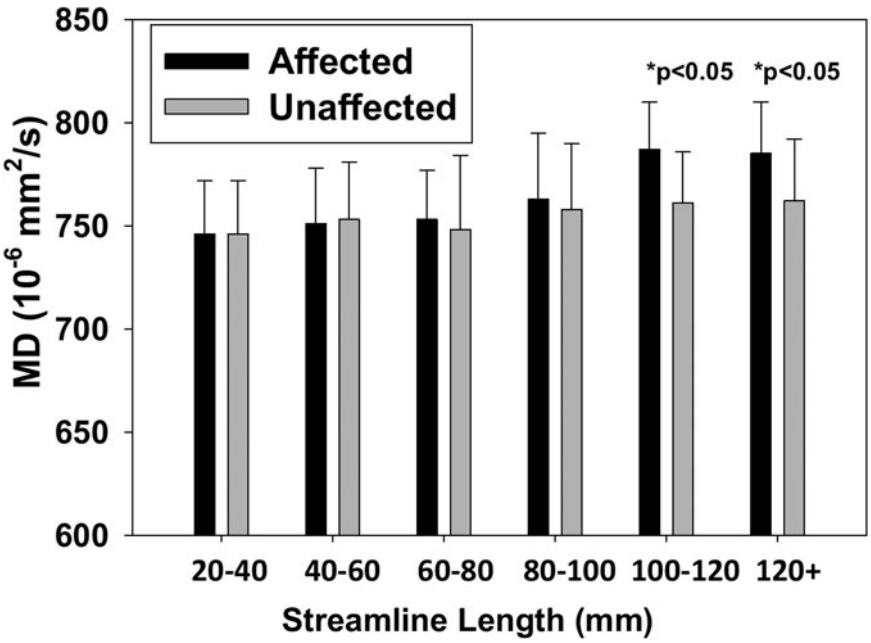

FIG. 5. Comparison of MD between the affected and unaffected tracts across lengths. The bar and error bar denote the average and standard deviation across the concussed athletes, respectively. Paired *t*-tests were used to compare the mean MD along the fiber streamlines between the affected and unaffected tracts for each length category. MD, mean diffusivity.

Regardless of the length, the mean MD along the unaffected tracts was approximately 750×10^{-6} mm^2/sec, similar to the MD value along the short streamlines in the affected tracts (Fig. 5). Along the affected tracts, long streamlines (>100 mm) had a significantly higher average MD of 780×10^{-6} mm^2/sec ($ps<0.05$) compared with streamlines of the same length along unaffected tracts in the concussed athletes. In addition, MD in the long affected tracts (>80 mm) demonstrated significant correlations ($p=0.015$, $r=0.732$) with one of the clinical assessment scores (i.e., BSI), whereas the short tracts were not significant ($p=0.063$; Fig. 6). This observation suggested that worse psychological distress as measured by the BSI may be associated with higher MD in the affected white-matter tracts among the concussed athletes. Other clinical assessments showed no significant associations in this study. Due to the exploratory nature of this study and potential high correlation among the five clinical assessments, multiple comparison adjustment was not performed.

Discussion

In the present study, we first identified a vulnerable white-matter region in the concussed athletes. In this region, the concussed athletes had significantly elevated mean diffusivity 24–48 h post-injury compared with the contact-sport controls. The anatomical location of this acute white-matter alteration was consistent with previous findings from different sample sizes or cohorts[28,29,31] and other studies.[23,25,30,56,57] Particularly, this vulnerable white-matter region was part of four major white-matter tracts (i.e., forceps minor, superior and posterior corona radiata, and cingulum) and demonstrated an acute increase in the freedom of water diffusion. The increase in MD covers a wider anatomical range than the RD. The underlying pathology of increased MD could be axonal swelling,[58] extracellular edema,[59] cytoskeleton breakdown,[58] demyelination,[60,61] or decreased viscosity in the plasma or extracellular matrix.[62] An increase in RD with unchanged longitudinal diffusivity suggests additional compromise in the transverse direction of axons, most likely from demyelination.[63]

In the four affected white-matter tracts, the histogram across length was significantly different from the whole-brain distribution. A whole-brain white-matter histogram over length usually demonstrates large numbers of short fiber streamlines. The number of streamlines decreases as the fiber length increases.[20,64] With higher prevalence of the short fibers, if propagating shear stress impacts the white-matter tissue by pure chance, one would expect a greater affected ratio in short fibers. This was not what we observed here. In fact, we observed a higher per-unit-length affected ratio in long fibers, suggesting specific physical or biological vulnerability of longer fibers. A possible biomechanical explanation for this observation is that the myelin sheath that accelerates action

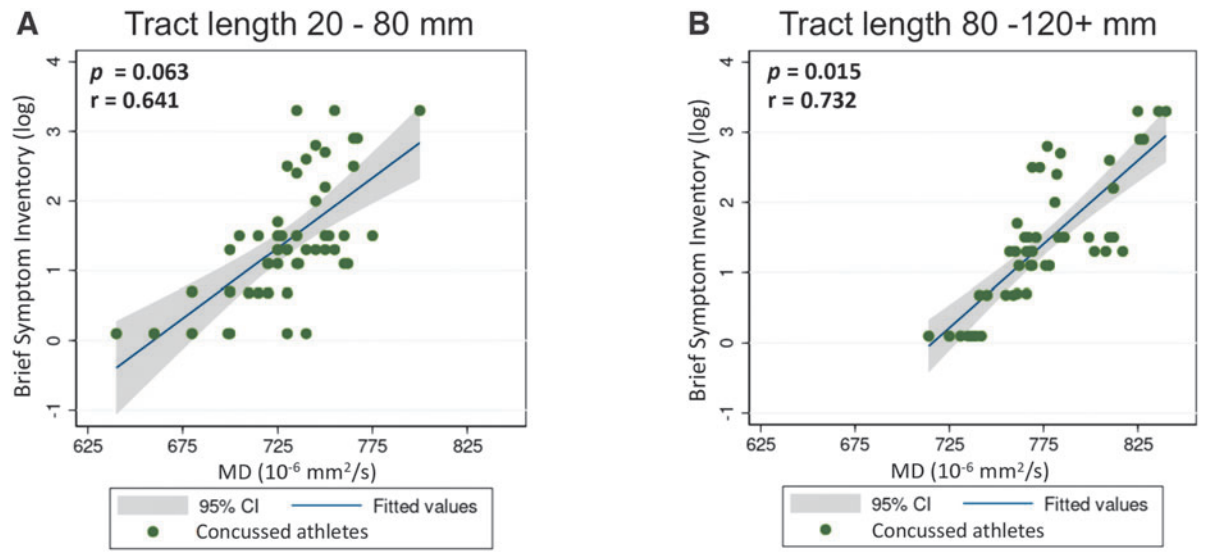

FIG. 6. Partial correlations between MD along the affected tracts and the BSI score. **(A)** The partial correlation between MD along the short streamlines (<80 mm) and the BSI score adjusted for sites and MRI scanner. **(B)** The partial correlation between MD along the long streamlines (>80 mm) and the BSI score adjusted for sites and MRI scanners. To adjust the skewness in the distributions, the BSI score was logarithmically transformed prior to correlating. Each dot represents one concussed athlete. BSI, Brief Symptom Inventory; MD, mean diffusivity; MRI, magnetic resonance imaging.

potentials in long fibers makes longer axons stiffer and more susceptible to shear stress and strain,[18,19,65] or that the central and deep location of long fiber tracts amplifies the shear and twisting force.[66,67] Future studies of large animals or cadavers with a realistic brain mass and shear stress may help to validate these hypotheses.

The vulnerability of long fiber tracts was further supported by two other independent measures. Along the fiber tract streamlines, long fibers had higher MD and significant associations with the clinical outcome measure, BSI. The increased MD suggests that microstructural changes were propagated along the whole tract in long fibers even beyond those focal points that had significant group differences. This finding also suggests that the tractography approach to identifying microstructural changes in long fibers may be more sensitive than conventional groupwise ROI or voxel-base analyses. A groupwise analysis searches for synchronized abnormalities and penalizes inter-subject variation, whereas the tract-specific analysis is an individualized and subject-specific analysis. Subject-specific analyses may be more sensitive in SRC, in which the uniqueness of brain injury arises from differences in the directionality and magnitude of biomechanical forces.[68,69]

Whereas ROI- or voxel-based analyses are used in most published DTI studies on SRC, individualized and tract-specific analyses are less well investigated[70] due to complex and computationally demanding data analyses. In white-matter tractography, data analyses require intense computation in generating tens of thousands of streamline profiles for each participant and converting Cartesian-coordinate scalar maps (e.g., FA, MD) into the streamline intrinsic coordinate. Nevertheless, diffusion MRI tractography is the only *in vivo* approach available for studying white-matter tracts in the brain.[71] Previous tractography studies in mild TBI focused on clinical association with diffusion metrics in few predefined tracts,[10,72,73] or on connectome network analyses.[74–76] To the best of our knowledge, this is the first study to provide objective evidence of vulnerability in terms of the physical features of white-matter fibers.

This study evaluating the effect of physical features in vulnerability of white matter after acute SRC has some limitations. The definition of affected and unaffected white matter was based on the TBSS analysis of group differences with corrected $p < 0.05$. Although the 0.05 criterion is widely used, it is an arbitrary threshold. Due to the likely continuum of concussion effects throughout the brain, different thresholds might yield different findings. Further, as pointed out in our previous publication,[28,29,31] despite a high degree of sensitivity, the biological interpretation of changes in DTI metrics remains challenging. Such limitation stems from trying to use a simplified diffusion tensor model to describe an ensemble effect of water diffusion in complex biological tissues, such as crossing fibers[71,77–80] or compartmentalization.[81,82] Therefore, to overcome the insufficiency of the second order proximate (i.e., the diffusion tensor),

spherical harmonic deconvolution (SHD),[83] q-ball imaging (QBI),[84] or Bayesian estimation[85] were proposed to estimate multiple crossing fibers. The finer granularity of diffusion compartments may be decomposed by diffusion modeling such as the composite hindered and restricted model of diffusion (CHARMED),[86] neurite orientation dispersion and density imaging (NODDI),[87] or diffusion kurtosis imaging (DKI).[88]

Although diffusion MRI tractography provides a convenient approach for evaluating white-matter fiber tracts non-invasively, its streamline results may vary across software tools. Because there are no standardized tractography software tools, this study utilized a reputable and well-maintained toolbox with default settings. The q-ball and spherical harmonic reconstruction for fiber orientation enabled crossing fiber estimation and high-quality seeds and destination also minimized the noise in tractography. Nevertheless, this study may still be limited by low angular sampling resolution, affecting the ability to fully resolve crossing, bending, or kissing fibers.

Another limitation of this study is the potential long-term effects of previous concussions. Previous injury history is an important factor in SRC. For this reason, the CARE study excludes participants who have concussions within 6 months prior to the baseline assessments. Also, participants with abnormal clinical assessment scores at baseline were excluded, meaning that all the participants are clinically recovered at the time of recruitment. We believe that these inclusion/exclusion criteria should minimize the lingering effects of previous concussions (if there are any) to the acute effects investigated in this study. Lastly, as an exploratory study with a limited sample size, multiple comparison adjustments were not performed for the analyses in Figures 5 and 6.

Conclusions

In this study by the CARE Consortium, we characterized the susceptibility of white-matter fiber tracts to SRC with respect to tract length. Fiber tracts longer than 100 mm appeared to be more vulnerable to this mild brain injury with higher MD and significant clinical correlations. These findings help further inform the pathophysiological mechanisms of concussion, which have important implications for understanding neurobiological recovery and possible development of therapeutic interventions to promote brain recovery after mild TBI.

Acknowledgments

Opinions, interpretations, conclusions, and recommendations are those of the author and are not necessarily endorsed by the Department of Defense.

The authors thank Jody Harland, MS, Janetta Matesan, BA, Michael Menser, Larry Riggen, MS (Indiana University School of Medicine); Ashley Rettmann, BS, Nicole L'Heureux, MBA (University of Michigan); Melissa Koschnitzke, MA (Medical College of Wisconsin); Michael Jarrett, MBA, Vibeke Brinck, MS, and Bianca Byrne, BA (Quesgen); Melissa Baker, BS (Datalys Center for Sports Injury Research and Prevention); and the research and medical staff at each of the CARE participation sites. We are grateful for the participation of the student athletes without whom this research would not be possible.

Authors' Contributions

S.M. Mustafi and H.C. Yang contributed data analyses and interpretation of data and results. T.B. Meier and B.L. Brett contributed critical revision of the manuscript for important intellectual content. C.C. Giza, J. Goldman, K.M. Guskiewicz, J.P. Mihalik, S.M. LaConte, and S.M. Duma contributed data acquisition and critical revision of the manuscript for important intellectual content. J. Harezlak contributed study concept and design, interpretation of data and results, and critical revision of the manuscript for important intellectual content. S.P. Broglio, M.A. McCrea, and T.W. McAllister contributed study concept and design and critical revision of the manuscript for important intellectual content. Y.C. Wu contributed data analyses, interpretation of data and results, drafting the manuscript for intellectual content, and critical revision of the manuscript for important intellectual content.

Funding Information

This publication was made possible, in part, with support from the Grand Alliance CARE Consortium, funded, in part by the NCAA and the DOD. The U.S. Army Medical Research Acquisition Activity, Fort Detrick, MD, is the awarding and administering acquisition office. This work was supported by the Office of the Assistant Secretary of Defense for Health Affairs, through the Combat Casualty Care Research Program, endorsed by the DOD, through the Joint Program Committee 6/Combat Casualty Care Research Program – Psychological Health and Traumatic Brain Injury Program under award number W81XWH1420151. Other funding supports include National Institutes of Health grant R01 NS112303 to Y.C.W. and J.H. and R01 AG053993 to Y.C.W.

Author Disclosure Statement

No competing financial interests exist.

Supplementary Material

Supplementary Figure S1
Supplementary Figure S2

References

1. Langlois JA, Rutland-Brown W, Wald MM. The epidemiology and impact of traumatic brain injury: a brief overview. J Head Trauma Rehabil 2006;21:375–378.
2. Daneshvar, DH, Nowinski, CJ, McKee, et al. The epidemiology of sport-related concussion. Clin Sports Med 2011;30:1–17, vii.
3. ICHD-3. (2018). The International Classification of Headache Disorders, 3rd edition. Cephalalgia.

4. McCrory P, Meeuwisse W, Dvorak J, et al. Consensus statement on concussion in sport-the 5(th) International Conference on Concussion in Sport held in Berlin, October 2016. Br J Sports Med 2017;51:838–847.
5. McCrea M, Broglio S, McAllister T, et al., CARE Consortium Investigators. Return to play and risk of repeat concussion in collegiate football players: comparative analysis from the NCAA Concussion Study (1999-2001) and CARE Consortium (2014-2017). Br J Sports Med 2019;54(2):102–109.
6. Manley G, Gardner AJ, Schneider KJ, et al. A systematic review of potential long-term effects of sport-related concussion. Br J Sports Med 51 2017;969–977.
7. McKee AC, Stern RA, Nowinski CJ, et al. The spectrum of disease in chronic traumatic encephalopathy. Brain 2013;136:43–64.
8. Levin B, Bhardwaj A. Chronic traumatic encephalopathy: a critical appraisal. Neurocrit Care 2014;20:334–344.
9. Silver JM, McAllister TW, Yudofsky SC (eds). Textbook of Traumatic Brain Injury. 3rd ed. American Psychiatric Pub: Washington, DC; 2018; p. 664.
10. Laskowitz D, Grant G (eds). (2016). Translational Research in Traumatic Brain Injury (Frontiers in Neuroscience Book 57). CRC Press: Boca Raton, FL; 2016; pp. xxii, 412.
11. Farkas O, Povlishock JT. Cellular and subcellular change evoked by diffuse traumatic brain injury: a complex web of change extending far beyond focal damage. Prog Brain Res 2007;161:43–59.
12. Buki A, Povlishock JT. All roads lead to disconnection? Traumatic axonal injury revisited. Acta Neurochir (Wien) 2006;148:181–193; discussion 193–184.
13. LaPlaca MC, Prado GR, Cullen D, et al. Plasma membrane damage as a marker of neuronal injury. Conf Proc IEEE Eng Med Biol Soc 2009:1113–1116.
14. Simon CM, Sharif S, Tan RP, et al. Spinal cord contusion causes acute plasma membrane damage. J Neurotrauma 2009;26:563–574.
15. Clayton EH, Genin GM, Bayly PV. Transmission, attenuation and reflection of shear waves in the human brain. J R Soc Interface 2012;9:2899–2910.
16. Wright RM, Post A, Hoshizaki B, et al. A multiscale computational approach to estimating axonal damage under inertial loading of the head. J Neurotrauma 2013;30:102–118.
17. Su E, Bell M. Diffuse Axonal Injury. In: Translational Research in Traumatic Brain Injury. (Laskowitz D, Grant G, eds.) CRC Press: Boca Raton, FL; 2016.
18. Smith DH, Wolf JA, Lusardi TA, et al. High tolerance and delayed elastic response of cultured axons to dynamic stretch injury. J Neurosci 1999;19:4263–4269.
19. Laksari K, Shafieian M, Darvish K. Constitutive model for brain tissue under finite compression. J Biomech 2012;45:642–646.
20. Bajada CJ, Schreiber J, Caspers S. Fiber length profiling: a novel approach to structural brain organization. Neuroimage 2019;186:164–173.
21. Zhang L, Heier LA, Zimmerman RD, et al. Diffusion anisotropy changes in the brains of professional boxers. AJNR Am J Neuroradiol 2006;27:2000–2004.
22. Cubon VA, Putukian M, Boyer C, et al. A diffusion tensor imaging study on the white matter skeleton in individuals with sports-related concussion. J Neurotrauma 2011;28:189–201.
23. Henry LC, Tremblay J, Tremblay S, et al. Acute and chronic changes in diffusivity measures after sports concussion. J Neurotrauma 2011;28:2049–2059.
24. Bazarian JJ, Zhu T, Blyth B, et al. Subject-specific changes in brain white matter on diffusion tensor imaging after sports-related concussion. Magn Reson Imaging 2012;30:171–180.
25. Koerte IK, Kaufmann D, Hartl E, et al. A prospective study of physician-observed concussion during a varsity university hockey season: white matter integrity in ice hockey players. Part 3 of 4. Neurosurg Focus 2012;33(E3):1–7.
26. Murugavel M, Cubon V, Putukian M, et al. A longitudinal diffusion tensor imaging study assessing white matter fiber tracts after sports-related concussion. J Neurotrauma 2014;31:1860–1871.
27. Lancaster MA, Olson DV, McCrea MA, et al. Acute white matter changes following sport-related concussion: a serial diffusion tensor and diffusion kurtosis tensor imaging study. Hum Brain Mapp 2016;37:3821–3834.
28. Wu YC, Mustafi SM, Harezlak J, et al. Hybrid diffusion imaging in mild traumatic brain injury. J Neurotrauma 2018;35:2377–2390.
29. Mustafi SM, Harezlak J, Koch KM, et al. Acute white-matter abnormalities in sports-related concussion: A diffusion tensor imaging study from the ncaa-dod care consortium. J Neurotrauma 2018;35:2653–2664.
30. McAllister TW, Ford JC, Flashman LA, et al. Effect of head impacts on diffusivity measures in a cohort of collegiate contact sport athletes. Neurology 2014;82:63–69.
31. Wu YC, Harezlak J, Elsaid NMH, et al. Longitudinal white-matter abnormalities in sports-related concussion: a diffusion MRI study. Neurology 2020;95:e781–e792.
32. Meier TB, Bergamino M, Bellgowan PS, et al. Longitudinal assessment of white matter abnormalities following sports-related concussion. Hum Brain Mapp 2016;37:833–845.
33. Hulkower MB, Poliak DB, Rosenbaum SB, et al. A decade of DTI in traumatic brain injury: 10 years and 100 articles later. AJNR Am J Neuroradiol 2013;34:2064–2074.
34. Eierud C, Craddock RC, Fletcher S, et al. Neuroimaging after mild traumatic brain injury: review and meta-analysis. Neuroimage Clin 2014;4:283–294.
35. Gardner A, Kay-Lambkin F, Stanwell P, et al. A systematic review of diffusion tensor imaging findings in sports-related concussion. J Neurotrauma 2012;29:2521–2538.
36. Dodd AB, Epstein K, Ling JM, et al. Diffusion tensor imaging findings in semi-acute mild traumatic brain injury. J Neurotrauma 2014;31:1235–1248.
37. Shenton ME, Hamoda HM, Schneiderman JS, et al. A review of magnetic resonance imaging and diffusion tensor imaging findings in mild traumatic brain injury. Brain Imaging Behav 2012;6:137–192.
38. Pan J, Connolly ID, Dangelmajer S, et al. Sports-related brain injuries: connecting pathology to diagnosis. Neurosurg Focus 2016;40:E14.
39. McCrea M, Meier T, Huber D, et al. Role of advanced neuroimaging, fluid biomarkers and genetic testing in the assessment of sport-related concussion: a systematic review. Br J Sports Med 2017;51:919–929.
40. Carney N, Ghajar J, Jagoda A, et al. (2014). Concussion guidelines step 1: systematic review of prevalent indicators. Neurosurgery 2014; 75(Suppl 1):S3–S15.
41. Broglio SP, McCrea M, McAllister T, et al., CARE Consortium Investigators. A national study on the effects of concussion in collegiate athletes and US military service academy members: the NCAA-DOD Concussion Assessment, Research And Education (CARE) Consortium structure and methods. Sports Med 2017;47:1437–1451.
42. Wechsler D. Manual for the Wechsler Adult Intelligence Scale (rev. ed.). The Pscyhological Corporation, Harcourt Brace Janvanovich, Inc.: New York; 1987.
43. McCrea M, Kelly JP, Randolph C. Standardized Assessment of Concussion (SAC): Manual for Administration, Scoring and Interpretation. CNS Inc.: Waukesha, WI; 1996.
44. Guskiewicz KM, Ross SE, Marshall SW. Postural stability and neuropsychological deficits after concussion in collegiate athletes. J Athl Train 2001;36:263–273.
45. Derogatis LR. BSI Brief Symptom Inventory: Administration, Scoring, and Procedure Manual (4th ed.). National Computer Systems: Minneapolis, MN; 1993.
46. Nencka AS, Meier TB, Wang Y, et al. Stability of MRI metrics in the advanced research core of the NCAA-DOD Concussion Assessment, Research and Education (CARE) Consortium. Brain Imaging Behav 2018;12:1121–1140.
47. Lepage C, de Pierrefeu A, Koerte IK, et al. White matter abnormalities in mild traumatic brain injury with and without post-traumatic stress disorder: a subject-specific diffusion tensor imaging study. Brain Imaging Behav 2018;12:870–881.
48. Manjon JV, Coupe P, Concha L, et al. Diffusion weighted image denoising using overcomplete local PCA. PLoS One 2013;8:e73021.
49. Andersson JL, Sotiropoulos SN. An integrated approach to correction for off-resonance effects and subject movement in diffusion MR imaging. Neuroimage 2016;125:1063–1078.
50. Basser PJ, Mattiello J, LeBihan D. MR diffusion tensor spectroscopy and imaging. Biophys J 1994;66:259–267.
51. Avants BB, Tustison NJ, Song G, et al. A reproducible evaluation of ants similarity metric performance in brain image registration. Neuroimage 2011;54:2033–2044.
52. Cook, PB, Y; Nedjati-Gilani, S; Seunarine, KK; Hall, MG; Parker, GJ; Alexander, DC. Camino: Open-source diffusion-mri reconstruction and processing. In: ISMRM. 2006. Seattle, WA, USA.
53. Smith SM, Jenkinson M, Johansen-Berg H, et al. Tract-based spatial statistics: voxelwise analysis of multi-subject diffusion data. Neuroimage 2006;31:1487–1505.
54. Smith SM, Nichols TE. Threshold-free cluster enhancement: addressing problems of smoothing, threshold dependence and localisation in cluster inference. Neuroimage 2009;44:83–98.
55. Nichols TE, Holmes AP. Nonparametric permutation tests for functional neuroimaging: a primer with examples. Hum Brain Mapp 2002;15:1–25.

56. Chamard E, Lassonde M, Henry L, et al. Neurometabolic and microstructural alterations following a sports-related concussion in female athletes. Brain Inj 2013;27:1038–1046.
57. Lancaster MA, Meier TB, Olson DV, et al. Chronic differences in white matter integrity following sport-related concussion as measured by diffusion MRI: 6-month follow-up. Hum Brain Mapp 2018;39:4276–4289.
58. Pierpaoli C, Barnett A, Pajevic S, et al. Water diffusion changes in wallerian degeneration and their dependence on white matter architecture. Neuroimage 2001;13:1174–1185.
59. Kinoshita M, Goto T, Okita Y, et al. Diffusion tensor-based tumor infiltration index cannot discriminate vasogenic edema from tumor-infiltrated edema. J Neurooncol 2010;96:409–415.
60. Rocca MA, Sonkin M, Copetti M, et al. Diffusion tensor magnetic resonance imaging in very early onset pediatric multiple sclerosis. Mult Scler 2016;22:620–627.
61. Wu YC, Field AS, Duncan ID, et al. High b-value and diffusion tensor imaging in a canine model of dysmyelination and brain maturation. Neuroimage 2011;58:829–837.
62. Westlye LT, Walhovd KB, Dale AM, et al. Life-span changes of the human brain white matter: diffusion tensor imaging (DTI) and volumetry. Cereb Cortex 2010;20:2055–2068.
63. Song SK, Sun SW, Ramsbottom MJ, et al. Dysmyelination revealed through MRI as increased radial (but unchanged axial) diffusion of water. Neuroimage 2002;17:1429–1436.
64. Lichenstein SD, Bishop JH, Verstynen TD, et al. Diffusion capillary phantom vs. human data: outcomes for reconstruction methods depend on evaluation medium. Front Neurosci 2016;10:407.
65. Metz H, McElhaney J, Ommaya AK. A comparison of the elasticity of live, dead, and fixed brain tissue. J Biomech1970;3:453–458.
66. Bayly PV, Cohen TS, Leister EP, et al. (2005). Deformation of the human brain induced by mild acceleration. J Neurotrauma 2005;22:845–856.
67. Viano DC, Casson IR, Pellman EJ, et al. Concussion in professional football: brain responses by finite element analysis: part 9. Neurosurgery 2005;57:891–916; discussion 891–916.
68. Mac Donald CL, Johnson AM, Cooper D, et al. Detection of blast-related traumatic brain injury in U.S. military personnel. N Engl J Med 2011;364:2091–2100.
69. Lipton ML, Kim N, Park YK, et al. Robust detection of traumatic axonal injury in individual mild traumatic brain injury patients: intersubject variation, change over time and bidirectional changes in anisotropy. Brain Imaging Behav 2012;6:329–342.
70. Narayana PA. White matter changes in patients with mild traumatic brain injury: MRI perspective. Concussion 2017;2:CNC35.
71. Jones DK. Studying connections in the living human brain with diffusion MRI. Cortex 2008;44:936–952.
72. Wilde EA, McCauley SR, Barnes A, et al. Serial measurement of memory and diffusion tensor imaging changes within the first week following uncomplicated mild traumatic brain injury. Brain Imaging Behav 2012;6:319–328.
73. Wilde EA, Li X, Hunter JV, et al. Loss of consciousness is related to white matter injury in mild traumatic brain injury. J Neurotrauma 2016;33:2000–2010.
74. Iraji A, Chen H, Wiseman N, et al. Connectome-scale assessment of structural and functional connectivity in mild traumatic brain injury at the acute stage. Neuroimage Clin 2016;12:100–115.
75. Dall'Acqua P, Johannes S, Mica L, et al. Connectomic and surface-based morphometric correlates of acute mild traumatic brain injury. Front Hum Neurosci 2016;10:127.
76. Dall'Acqua P, Johannes S, Mica L, et al. Functional and structural network recovery after mild traumatic brain injury: a 1-year longitudinal study. Front Hum Neurosci 2017;11:280.
77. Wheeler-Kingshott CA, Cercignani M. About "axial" and "radial" diffusivities. Magn Reson Med 2009;61:1255–1260.
78. Alexander AL, Hasan KM, Lazar M, et al. Analysis of partial volume effects in diffusion-tensor MRI. Magn Reson Med 2001;45:770–780.
79. Wu YC, Diffusion MRI: Tensors and Beyond. In: Medical Physics. University of Wisconsin-Madison: Madison, WI; 2006; p. 150.
80. Tournier JD, Mori S, Leemans A. Diffusion tensor imaging and beyond. Magn Reson Med 2011;65:1532–1556.
81. Assaf Y, Pasternak, O. Diffusion tensor imaging (DTI)-based white matter mapping in brain research: a review. J Mol Neurosci 2008;34:51–61.
82. Jones DK, Knosche TR, Turner R. White matter integrity, fiber count, and other fallacies: the do's and don'ts of diffusion MRI. Neuroimage 2013;73:239–254.
83. Tournier JD, Yeh CH, Calamante F, et al. Resolving crossing fibres using constrained spherical deconvolution: validation using diffusion-weighted imaging phantom data. Neuroimage 2008;42:617–625.
84. Tuch DS. Q-ball imaging. Magn Reson Med 2004;52:1358–1372.
85. Behrens TE, Berg HJ, Jbabdi S, et al. Probabilistic diffusion tractography with multiple fibre orientations: what can we gain? Neuroimage 2007;34:144–155.
86. Assaf Y, Basser PJ. Composite hindered and restricted model of diffusion (CHARMED) MR imaging of the human brain. Neuroimage 2005;27:48–58.
87. Zhang H, Schneider T, Wheeler-Kingshott CA, et al. Noddi: practical in vivo neurite orientation dispersion and density imaging of the human brain. Neuroimage 2012;61:1000–1016.
88. Fieremans E, Jensen JH, Helpern JA. White matter characterization with diffusional kurtosis imaging. Neuroimage 2011;58:177–188.